MULTICARRIER CHIP PULSE SHAPE DESIGN WITH LOW PAPR

Mariano Vergara, Felix Antreich

German Aerospace Center (DLR)
Institute for Communications
and Navigation
82234 Wessling, Germany
email:{mariano.vergara,
felix.antreich}@dlr.de

Gonzalo Seco-Granados[*]

SPCOMNAV
Department of Telecommunications
and Systems Engineering
Universitat Autónoma de Barcelona (UAB)
08193 Bellatera (Barcelona), Spain
email: gonzalo.seco@uab.es

ABSTRACT

In this paper we present a methodology to design pulse shapes for a direct sequence code division multiple access (DS-CDMA) ranging signal, using a multicarrier (MC) modulation. The advantage of this signal design methodology is that it allows us to perform spectral shaping with very low Peak-to-Average-Power Ratio (PAPR). This feature makes this approach very interesting for ranging systems for which flexible resource allocation and power efficiency are major concerns, e.g. GNSS (Global Navigation Satellite Systems).

Index Terms— Multicarrier ranging signal, low PAPR, chip pulse shape design.

1. INTRODUCTION

Chip pulse shape design for direct sequence code division multiple access (DS-CDMA) systems has a major impact on many aspects of the ranging performance of a DS-CDMA system [1]. Moreover, a good chip pulse shape design can incorporate new services ensuring full backward compatibility with legacy users [2]. More in general, a modern signal design can reallocate the available resources, i.e. power and bandwidth, to fully match the demands of quickly evolving market scenarios, with the minimal impact on the transmitter and receiver hardware.

Multicarrier (MC) modulations offer flexible allocation of the bandwidth, where the controllable radio resources are the sub-bands which the available bandwidth is divided into. It is well known however that MC modulations can have higher Peak-to-Average Power Ratios (PAPR) than single carrier modulations. High PAPR values create problems when the ranging signal passes through mixers and nonlinear components such as a High Power Amplifier (HPA), causing power inefficiencies. In some applications where power efficiency plays a major role, e.g. Global Navigation Satellite Systems (GNSS), MC signals with a very low PAPR can be of great practical interest. Several methods have been proposed to reduced the PAPR of MC signals [3] for data transmission. Nevertheless, reducing the PAPR of unmodulated multitone signals, which can be used for ranging purposes, is a problem with different challenges [4] [5], which has not been as widely investigated as the problem of PAPR minimization for multitone signals aimed at data transmission. Since the PAPR minimization for MC signals used for ranging need not be done in real-time, more sophisticated, time-consuming algorithms can be implemented.

In this paper we present a new methodology to design the pulse shape of a DS-CDMA signal, employing a MC modulation with very low PAPR. This approach is based on the application of some codes developed more than half a century ago for radar pulse compression [6], and it allows to shape the Power Spectral Density (PSD) of the ranging signal, with the side constraint that the PAPR can never exceed 3 dB. This holds for any number of subcarriers. As a case study, in this paper we show how a MC chip pulse shape can have almost the same power spectrum of a pulse shape used for GNSS, namely a filtered BOCsin(1,1) signal [7], and yet have a PAPR which is roughly 1.5 dB lower. This suggests that the proposed chip-pulse shape design, besides offering high spectral flexibility and power efficiency, it offers a certain degree of backward compatibility.

2. SIGNAL MODEL

The chip pulse shape of a DS-CDMA signal can be parameterized as windowed multitone signal:

$$p(t) = \frac{1}{T_c} \underbrace{\sum_{n=0}^{N-1} c_n e^{j2\pi n \Delta_f t}}_{m(t)} \text{rect}\left(\frac{t}{T_c}\right) \quad , \qquad (1)$$

where $\text{rect}\left(\frac{t}{T_c}\right)$ indicates the rectangular function centered at 0 and of width equal to T_c, with T_c being the chip pulse duration in seconds. The chip pulse shape (1) is a complex multitone pulse created by windowing of the complex multitone signal $m(t)$. The frequency separation among the tones constituting the chip pulse $p(t)$ is given by Δ_f.

The complex vector

$$\mathbf{c} = [c_0, c_1, \ldots, c_{N-1}]^{\text{T}} \in \mathbb{C}^{N \times 1}, \qquad (2)$$

is called the *frequency code* of the multitone signal and it determines the amplitudes and the phases of N complex exponentials constituting the signal. We say that the multitone signal (1) is generated by a frequency code $\mathbf{c}$. A frequency code uniquely determines a pulse shape (1). In the following, we assume that the frequency code has unitary norm:

$$||\mathbf{c}||_2^2 = 1 \quad , \qquad (3)$$

which implies that the pulse (1) has unitary energy, if $\Delta_f = \frac{k}{T_c}$, $k \in N$. The frequency code can be written as

$$\mathbf{c} = \boldsymbol{\rho} \odot \boldsymbol{\theta}, \qquad (4)$$

where $\odot$ is the Hadamard-Schur product and

$$\boldsymbol{\rho} = [|c_0|, |c_1|, \ldots, |c_{N-1}|]^{\text{T}} \in \mathbb{R}^{N \times 1}, \qquad (5)$$

$$\boldsymbol{\theta} = [e^{j \arg\{c_0\}}, e^{j \arg\{c_1\}}, \ldots, e^{j \arg\{c_{N-1}\}}]^{\text{T}} \in \mathbb{R}^{N \times 1}, \qquad (6)$$

are respectively the code envelope and the phase vector of the frequency code $\mathbf{c}$. The vector $\boldsymbol{\rho}$ must fulfill the condition:

$$\rho_0 \rho_{N-1} = |c_0| |c_{N-1}| \neq 0. \qquad (7)$$

If this condition is not fulfilled, either the first or the last element of the frequency code, or both, are zero. This means that one or two subcarriers at the side of the spectrum contain no power, and thus they do not exist. Consequently, these subcarriers without power can be eliminated and thus instead of N, we will have $N-1$ or $N-2$ subcarriers. If the new subcarriers at the edges of the frequency code still have zero power, the frequency code can be further shortened. We say that a multitone signal possesses N subcarriers, when the frequency code cannot be further shortened, i.e. when (7) holds.

PSD of the signal (1) is mostly determined by the vector $\boldsymbol{\rho}$, that indicates how the power is divided among the subcarriers.

3. PROBLEM STATEMENT

Our objective is to shape the spectral content of $p(t)$ in a certain way, and at the same time we want $p(t)$ to have a small PAPR. That is, we intend to determine the vector $\boldsymbol{\rho}$ so that the PSD of the pulse shape fits a certain spectral mask and

we want to calculate the vector $\boldsymbol{\theta}$ that for this $\boldsymbol{\rho}$ minimizes the PAPR. Since $p(t)$ is a strictly time-limited pulse, a DS-CDMA signal built with the pulse $p(t)$ and spread with a constant envelope spreading code has the same PAPR as $p(t)$. Determining $\boldsymbol{\theta}$ for a given $\boldsymbol{\rho}$ such that the PAPR is minimal is already a very challenging problem for which only empirical or numerical solutions (e.g. [8]) have been proposed. In this work, we want to solve this problem jointly with the optimization of the vector $\boldsymbol{\rho}$.

The PAPR of the pulse $p(t)$ generated by the generic frequency code $\mathbf{c}$, which for simplicity will also be called the PAPR of the frequency code $\mathbf{c}$, is given by

$$\text{PAPR}_{\mathbf{c}} = \frac{\max_t \left\{ |p(t)|^2 \right\}}{\frac{1}{T_c} \int_{T_c} |p(t)|^2 \mathrm{d}t}, \qquad (8)$$

The relationship between the frequency code and the PAPR of the corresponding pulse can be described by means of the aperiodic auto-correlation function of the frequency code, as we show. Let the aperiodic auto-correlation of the frequency code $\mathbf{c}$ be

$$r_{\mathbf{c}}[d] = \begin{cases} \sum_{k=0}^{N-d-1} c_{k+d} \, c_k^* , & d < 0 \\ \\ \sum_{k=0}^{N+d-1} c_k \, c_{k-d}^* , & d \geq 0 \end{cases} \qquad (9)$$

The instantaneous power of the pulse (1) can be expressed as

$$|p(t)|^2 = 1 + 2 \, \Re \left\{ \sum_{d=1}^{N-1} r_{\mathbf{c}}[d] e^{j2\pi d\Delta_f t} \right\}, \qquad (10)$$

Since the frequency code has unitary energy we can state that:

$$\text{PAPR}_{\mathbf{c}} = 1 + 2 \sum_{d=1}^{N-1} \left| r_{\mathbf{c}}[d] \right| \cos\left(2\pi d\Delta_f t + \arg\{r_{\mathbf{c}}[d]\} \right) \qquad (11)$$

It is possible to prove [9, Appendix] that:

$$\sum_{d=1}^{N-1} \left| r_{\mathbf{c}}[d] \right|^2 \longrightarrow 0 \; \overset{m.s.}{\Longleftrightarrow} \; PAPR_{\mathbf{c}} \longrightarrow 0 \, \text{dB} \qquad (12)$$

with $\overset{m.s.}{\Longleftrightarrow}$ indicating a convergence in the mean square sense.

Minimizing the metric:

$$\sum_{d=1}^{N-1} \left| r_{\mathbf{c}}[d] \right|^2 \qquad (13)$$

minimizes the maximum possible PAPR [10], yet this does not allow a full control on the PAPR of the MC signal, because the convergence (12) holds only in the mean square sense. Moreover, since the convergence (12) holds only in the mean square sense, a frequency code that generates a MC signal with a small PAPR does not necessarily have a small value

of the metric (13) [11]. On top of that, the metric (13) depends both on the vector $\boldsymbol{\rho}$ and the vector $\boldsymbol{\theta}$; while the vector $\boldsymbol{\theta}$ in principle can be devoted entirely to PAPR minimization, the vector $\boldsymbol{\rho}$ must jointly optimise both the spectral shape and the PAPR and this constitutes a very challenging task.

This non-trivial problem can be significantly simplified if all the coefficients of the aperiodic autocorrelation of the frequency code, except the first and the last ones, are set to zero:

$$\left| r_{\mathbf{c}}[d] \right| = 0, \qquad d = 1, 2, \ldots, N-2 \quad . \tag{14}$$

If condition (14) is fulfilled by a frequency code $\mathbf{c}$, then the respective MC signal (and thus pulse) achieves the Friese's bound on the PAPR of a multitone signal [9]. A corollary to (14) is [6]:

$$\left| r_{\mathbf{c}}[N-1] \right| \leq 0.5 \quad . \tag{15}$$

Let any frequency code that fulfills condition (14) be denoted by $\mathbf{c}^{\dagger} = \boldsymbol{\rho}^{\dagger} \odot \boldsymbol{\theta}^{\dagger}$ and its aperiodic autocorrelation by $r_{\mathbf{c}^{\dagger}}[n]$. A code $\mathbf{c}^{\dagger}$ has the following properties:

1. The PAPR depends on a single parameter $\left| r_{\mathbf{c}^{\dagger}}[N-1] \right|$ and thus it can be easily steered.

2. The PAPR can never exceed 3 dB, independently from the number of subcarriers.

3. For a given value of $\left| r_{\mathbf{c}^{\dagger}}[N-1] \right|$ a limited number of codes $\mathbf{c}^{\dagger}$ exists [6].

The PAPR of codes fulfilling (14) is given by:

$$\gamma = 10 \log_{10} \left(1 + 2 \left| r_{\mathbf{c}^{\dagger}}[N-1] \right| \right) \quad , \tag{16}$$

which in conjunction with (15) explains why the PAPR is limited to 3 dB.

Moreover, it is worth noting that the PAPR minimization problem (e.g. [8]): "Given a vector $\boldsymbol{\rho}$, find the vector $\boldsymbol{\theta}$ that minimizes the objective function (8)" is not a problem that always possesses a global minimum. It is possible to prove that condition (14) restricts the set of all code envelopes to those vectors $\boldsymbol{\rho}$ for which there exists a vector $\boldsymbol{\theta}$ that provides a global minimum for the PAPR minimization problem. In the following we explain how to generate codes fulfilling condition (14) and how constrained spectral shaping can be performed.

4. HUFFMAN CODES

Condition (14) identifies a set of codes known as Huffman codes [6]. Huffman codes [6] are codes developed for radar pulse compression and are not to be confused with eponymous codes used for source data compression.

A Huffman code of length N is uniquely identified by two parameters

- a vector of $N-1$ binary symbols, which we call *binary generator* and indicate by $\mathbf{b}_k$, with the subscript k being the identifier of the binary generator,

- the sidelobe of the aperiodic correlation, that determines PAPR of the corresponding MC signal through (16).

The sidelobe of the aperiodic correlation $\left| r_{\mathbf{c}^{\dagger}}[N-1] \right|$ determines the two radii of the circles on which the $N-1$ roots of the associated polynomial are located [6]. The binary vector $\mathbf{b}_k$ determines, for each of the $N-1$ angular locations [6], on which of the two radii the roots of the k-th Huffman code are located. A cyclic permutation of the binary generator corresponds to a rotation of the roots. This operation corresponds to a multiplication for a complex exponential in the Huffman code space and it is thus irrelevant [12]. Two binary generators, which have the property that one cannot be written as a cyclic permutation of the other, individuate two different Huffman codes with distinct envelopes (5). Two Huffman codes with this property are said to be *distinct*, and such are their binary generators. Two distinct Huffman codes that have the same value of aperiodic correlation sidelobe $\left| r_{\mathbf{c}^{\dagger}}[N-1] \right|$ generate two MC pulses (1) with exactly the same PAPR. The set of all distinct Huffman codes that have the same aperiodic autocorrelation sidelobe represents the set of all possible codes satisfying (14) that yield the same PAPR. A Huffman code family is identified by the code length and the aperiodic autocorrelation sidelobe (or equivalently the PAPR γ). The generic Huffman code is indicated by $\mathbf{c}^{Huff}(\mathbf{b}_k, \gamma)$, where $\mathbf{b}_k$ is the binary generator identifying the code. The number of codes for each family is given by the number of the distinct binary generators. Spectral shaping is thus performed by means of a line search in all Huffman code families, in order to find the code $\mathbf{c}^{Huff}(\mathbf{b}_k, \gamma)$ with the desired code envelope. In particular:

1. All distinct binary vectors of length $N-1$ are generated.

2. For each value of the aperiodic autocorrelation sidelobe (between 0 and $\frac{1}{2}$), each binary vector generates a distinct Huffman code (with a distinct PSD).

3. The PSD of each distinct Huffman code is inspected and its fitting to the required spectral shaping criteria is assessed.

The line search is performed along two dimensions: the binary generators vectors $\mathbf{b}_k$, that form a finite countable set, and the aperiodic autocorrelation sidelobe, which forms an uncountable set. Making the search grid of the values of the aperiodic autocorrelation sidelobe dense enough, one can be sure of having inspected all chip pulse shapes (1) with the minimal theoretical PAPR (Friese's bound (16) [9]).

5. PROOF OF CONCEPT: GNSS SIGNALS

Using the method described above, a low-PAPR multitone pulse (1) can be adapted to match any spectral mask. In this section we show how such a signal can be used to match a BOC (Binary Offset Carrier) pulse, used in GNSS. This is technically relevant because it shows that signals developed with this approach can be backward compatible. As a secondary point, in this section we want also to highlight how BOC signals are a particular case of the signal (1).

GNSS signals are based on BOC modulation [13] to shape the pulse of the DS-CDMA signals used for ranging. BOC signals have been chosen for GNSS because of their capability to achieve adequate spectral separation with other GNSS signals in the same frequency band and for their low PAPR. BOC signals modulate a rectangular pulse with a square wave subcarriers, instead of a sinusoidal subcarrier, so that the signal envelope is constant, provided the number of the harmonics of the square wave is infinite. In this section we show that a MC pulse of the kind (1) can be shaped so that its PSD is very similar to the PSD of a BOCsin(1,1) [7] and yet have a smaller PAPR. A BOCsin(1,1) can be seen as a Manchester pulse [14, p.55]. In this example we consider an alternative version of a BOCsin(1,1), obtained by representing a BOCsin(1,1) with the model (1), and using a finite number of harmonics (i.e. subcarriers). According to this representation, a BOCsin(1,1) can be seen as a signal of the kind (1) whose frequency code is

$$
c_n^{BOC} = \begin{cases} -j\frac{2}{\pi n}, & \text{n odd}, \\ \\ 0, & \text{n even} \end{cases} \quad (17)
$$

This representation suggests also a flexible and power efficient approach to generate representations of BOC signals on the satellite payload. If the length of the frequency code is infinite, we obtain exactly the BOCsin(1,1) as defined in [7]. In this example we consider only 40 harmonics (20 without the null harmonics) from $n = -19$ till $n = 19$. The chip duration is $T_c = 0.977\mu sec$. The frequency separation among the non-zero harmonics is chosen equal to $\Delta_f = \frac{2}{Tc} = 2.046$ MHz. The frequency code identifying the BOCsin(1,1) pulse contains $N = 20$ non-zero elements.

Next, we consider Huffman codes of length $N = 20$ and we choose a frequency separation equal to $\Delta_f = \frac{2}{T_c}$. In order to perform spectral shaping of the MC pulse (1), we have to define a metric. Let $\boldsymbol{\rho}^{BOC}$ indicate the code envelope of the code (17) and $\boldsymbol{\rho}^{Huff}(\mathbf{b}_k, \gamma)$ the envelope of the Huffman code of the same length, generated by the generator $\mathbf{b}_k$ and with PAPR equal to γ dB. Since the PSD of a MC pulse (1) depends predominantly on the code envelope, we look for the Huffman code whose envelope has the smallest Euclidean distance from the envelope of the BOCsin(1,1) code (17). The best matching Huffman code is thus the one whose envelope

is

$$
\boldsymbol{\rho}_{opt}^{Huff} = \underset{\boldsymbol{\rho}^{Huff}(\mathbf{b}_k, \gamma)}{\operatorname{argmin}} \left\{ \left\| \boldsymbol{\rho}^{Huff}(\mathbf{b}_k, \gamma) - \boldsymbol{\rho}^{BOC} \right\|_2^2 \right\} \quad (18)
$$

For each value of γ, 4862 Huffman codes exist. The optimum Huffman code has a PAPR $\gamma = 0.015$ dB. A BOCsin(1,1) with 20 non-zero harmonics (corresponding to roughly a 10 MHz one-sided bandwidth) has a PAPR equal to 1.52 dB. The PSD of the BOCsin(1,1) and that of the optimized pulse are shown in Fig.1. As it can be observed, the PSD of the optimized MC signal is almost identical to the one of the BOCsin(1,1), and thus it could fulfill the current frequency regulations. The PAPR of the optimized MC pulse is one and a half dB lower. Also the magnitudes of the corresponding autocorrelation functions (Fig.2) are very similar too, with the optimized MC pulse having even a higher steepness around the main peak. The pulses can be observed in Fig.3.

The pulse optimised according the metric (18) has a correlation loss of roughly 1 dB with the BOC signal as defined in (17). This correlation loss comes, however, with the advantage of a smaller PAPR and thus of a higher transmit power efficiency. With some other metric this correlation loss may be made even smaller. As a closing remark, we would like to point out that the metric of this example has been chosen because it highlights the similarity between existing BOC pulse shapes and a more general way of designing low PAPR chip pulse shapes for DS-CDMA signals.
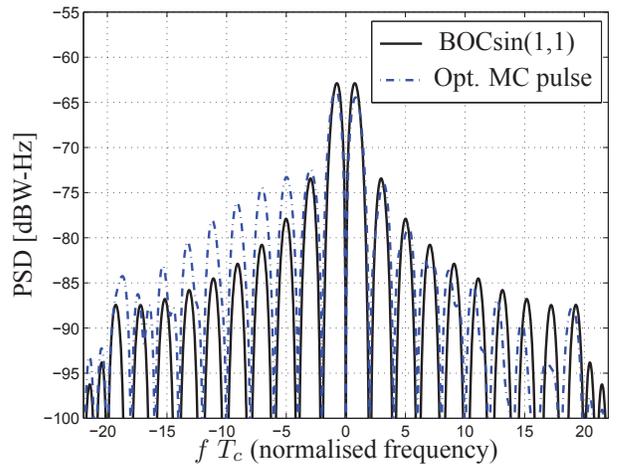
Fig. 1. Power Spectral Densities (PSD).

6. CONCLUSIONS

In this paper we have presented a methodology to design a chip pulse shape for a DS-CDMA ranging signal. This chip pulse pulse design approach is based on a MC modulation and uses some codes developed for radar pulse compression
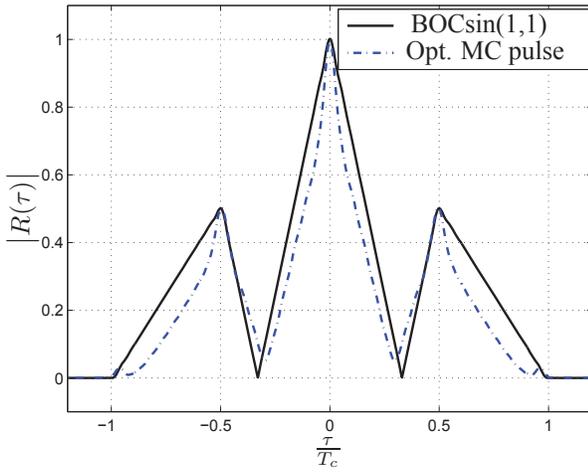
Fig. 2. Magnitudes of the pulse autocorrelation functions.
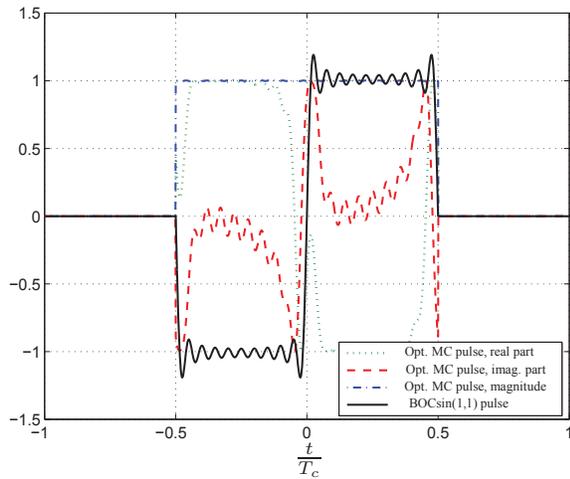
Fig. 3. Chip pulse shapes in time domain.

in order to have a deterministic control on the PAPR of the signal. This approach keeps the PAPR of the MC pulse very low (it can be at most 3 dB) for any number of subcarriers and thus it is of great interest for the design of ranging signals for systems that must be highly power efficient. As an example, the proposed approach was applied for GNSS ranging signal design and the optimized signal showed an extremely low PAPR (0.015 dB). With the proposed approach for ranging signal design high flexibility and high power efficiency, which are important future drivers for evolution of GNSS, can be achieved. Moreover the new chip pulse design approach can also be backward compatible to current GNSS signals.

7. REFERENCES

[1] F.Antreich and J.A. Nossek, "Optimum chip pulse shape design for timing synchronization," in *in Proceedings of the IEEE International Conference on Acoustics, Speech, and Signal Processing, ICASSP 2011*, Prague, Czech Republic, May 2011.

[2] F. Antreich, J.-L. Issler J.-J. Floch, and J. A. Nossek, "On backward compatibility in gnss signal design," in *in Proceedings of 6th European Workshop on GNSS Signals and Signal Processing, GNSS SIGNALS*, Toulouse, France, December 2011.

[3] S.H. Han and J. H. Lee, "An overview of peak-to-average power ratio reduction techniques for multicarrier transmission," *IEEE Wireless Communication Magazine*, pp. pp. 56–65, April 2005.

[4] S. Boyd, "Multitone signals with low crest factor," *IEEE Trans. Circuits Syst.*, vol. CAS-33, pp. 1018–1022, Otcober 1986.

[5] D. R. Gimlin, "On Minimizing the Peak-to-Average Power Ratio for the Sum of N Sinusoids," *IEEE Trans. on Communiations*, vol. 41, no. 4, April 1993.

[6] D. A. Huffman, "The generation of impulse equivalent pulse trains," *IRE. Trans. Inform. Theory*, vol. ITS, no. 5, pp. 10–16, 1962.

[7] "European GNSS (Galileo) Open Service, OS ICD, Issue 1," Tech. Rep., February 2010.

[8] M. R. Schroeder, "Synthesis of low-peak-factor signals and binary sequences with low autocorrelation," *IEEE Trans. Inform. Theory (Corresp.)*, vol. IT-16, pp. 85–89, June 1970.

[9] M.Friese, "Multitone signals with low crest factorsfriese," *IEEE Trans. on communications*, vol. 45, no. 10, October 1997.

[10] C. Tellambura, "Upper bound on peak factor of n-multiple carriers," *Elett. Letters*, vol. 33, pp. 185–187, Sept. 1997.

[11] N.Y. Ermolova and P. Vainikainen, "On the relationship between peak factor of a multicarrier signal and aperiodic autocorrelation of the generating sequence," *IEEE Comm. letters*, vol. 7, no. 3, pp. 107–108, 2003.

[12] L. Bomer and M. Antweiler, "Long energy efficient Huffman sequences," in *International Conference on Acoustics, Speech, and Signal Processing ICASSP-91*, April 1991, pp. 2905–2908.

[13] J.W. Betz, "Binary offset carrier modulations for radionavigation," *NAVIGATION: Journal of The Institute of Navigation*, vol. 48, no. 4, 2001.

[14] M.K. Simon, S.M. Hinedi, and W.C. Lindsey, *Digital Communication Techniques, Signal Design and Detection*, Pearson Education, Inc, 1995.